FULL PAPER

Magnetic Resonance in Medicine 00:00–00 (2016)

Black-Blood Native T_1 Mapping: Blood Signal Suppression for Reduced Partial Voluming in the Myocardium

Sebastian Weingärtner,[1,2,3]* Nadja M. Meßner,[1,4] Frank G. Zöllner,[1] Mehmet Akçakaya,[2,3] and Lothar R. Schad[1]

Purpose: To study the feasibility of black-blood contrast in native T_1 mapping for reduction of partial voluming at the blood–myocardium interface.

Methods: A saturation pulse prepared heart-rate-independent inversion recovery (SAPPHIRE) T_1 mapping sequence was combined with motion-sensitized driven-equilibrium (MSDE) blood suppression for black-blood T_1 mapping at 3 Tesla. Phantom scans were performed to assess the T_1 time accuracy. In vivo black-blood and conventional SAPPHIRE T_1 mapping was performed in eight healthy subjects and analyzed for T_1 times, precision, and inter- and intraobserver variability. Furthermore, manually drawn regions of interest (ROIs) in all T_1 maps were dilated and eroded to analyze the dependence of septal T_1 times on the ROI thickness.

Results: Phantom results and in vivo myocardial T_1 times show comparable accuracy with black-blood compared to conventional SAPPHIRE (in vivo: black-blood: 1562 $\pm$ 56 ms vs. conventional: 1583 $\pm$ 58 ms, $P = 0.20$); Using black-blood SAPPHIRE precision was significantly lower (standard deviation: 133.9 $\pm$ 24.6 ms vs. 63.1 $\pm$ 6.4 ms, $P < .0001$), and blood T_1 time measurement was not possible. Significantly increased interobserver interclass correlation coefficient (ICC) (0.996 vs. 0.967, $P = 0.011$) and similar intraobserver ICC (0.979 vs. 0.939, $P = 0.11$) was obtained with the black-blood sequence. Conventional SAPPHIRE showed strong dependence on the ROI thickness ($R^2 = 0.99$). No such trend was observed using the black-blood approach ($R^2 = 0.29$).

Conclusion: Black-blood SAPPHIRE successfully eliminates partial voluming at the blood pool in native myocardial T_1 mapping while providing accurate T_1 times, albeit at a reduced precision. **Magn Reson Med 000:000–000, 2016. © 2016 International Society for Magnetic Resonance in Medicine**

Key words: T_1 Mapping; SAPPHIRE; MSDE; black-blood; partial voluming

INTRODUCTION

Quantitative tissue characterization of the myocardium using cardiac MRI has emerged as a promising diagnostic tool with clinical value in numerous cardiomyopathies (1). Recently, native myocardial T_1 mapping has also shown prognostic value in pathologies with reduced myocardial wall thickness such as dilated cardiomyopathy (DCM) (2,3).

Myocardial T_1 mapping is commonly performed using a series of end-diastolic single-shot images acquired within a single breath hold (4,5). Variable magnetization preparation of the single-shot images induces varying T_1-weighted contrast and enables voxel-wise T_1 quantification.

However, the limited duration of the diastolic quiescence requires rapid imaging and restricts the in-plane resolution. This leads to major partial voluming effects at the myocardial–blood interface due to substantial differences in their respective T_1 times. Partial voluming reduces the myocardial area that is suitable for quantitative evaluation, impairs the reproducibility, and hampers the depiction of thin structures (6).

Segmented acquisition of the T_1-weighted images has been proposed to mitigate this shortcoming by improving the in-plane resolution (7–9). Similarly, T_1 quantification at systole has been proposed to increase the number of voxels within the myocardium that are not subject to partial voluming (10). However, residual partial voluming can still be expected even at higher resolutions or with increased myocardial wall thickness, especially in oblique orientations. Another approach to overcome this issue is blood suppression: In-flow saturation at the great vessels has been used to induce black-blood contrast (11) in the preclinical mouse model (12). Furthermore, a recent study presented preliminary data on the use of motion-sensitized driven-equilibrium (MSDE) (13) for black-blood T_1 mapping in humans (14). Both approaches achieved promising black-blood image quality but with reduced repeatability.

In this study, we sought to develop a MSDE-prepared black-blood native T_1 mapping method using combined saturation and inversion recovery magnetization preparation. Numerical simulations were performed to study the effects of blood suppression on partial voluming. Phantom scans and in vivo experiments in healthy volunteers were carried out to optimize the black-blood imaging parameters and to evaluate the proposed method on efficient blood signal suppression and homogeneous T_1 quantification.

[1]Computer Assisted Clinical Medicine, University Medical Center Mannheim, Heidelberg University, Mannheim, Germany.

[2]Electrical and Computer Engineering, University of Minnesota, Minneapolis, MN, United States.

[3]Center for Magnetic Resonance Research, University of Minnesota, Minneapolis, MN, United States.

[4]DZHK (German Centre for Cardiovascular Research) partner site Mannheim, Germany.

Grant sponsor: National Institutes of Health; Grant number: R00HL111410.

*Correspondence to: Dr. Sebastian Weingärtner, University Medical Center Mannheim, Theodor-Kutzer-Ufer 1-3, 68167 Mannheim, Germany.
E-mail: sebastian.weingaertner@medma.uni-heidelberg.de

COI: S.W. and M.A. are inventors of a pending U.S. and European patent entitled "Methods for scar imaging in patients with arrhythmia," which described the SAPPHIRE imaging sequence. No other financial or nonfinancial competing interests exist for any author.

Received 13 May 2016; revised 5 July 2016; accepted 20 July 2016

DOI 10.1002/mrm.26378

Published online 00 Month 2016 in Wiley Online Library (wileyonlinelibrary.com).

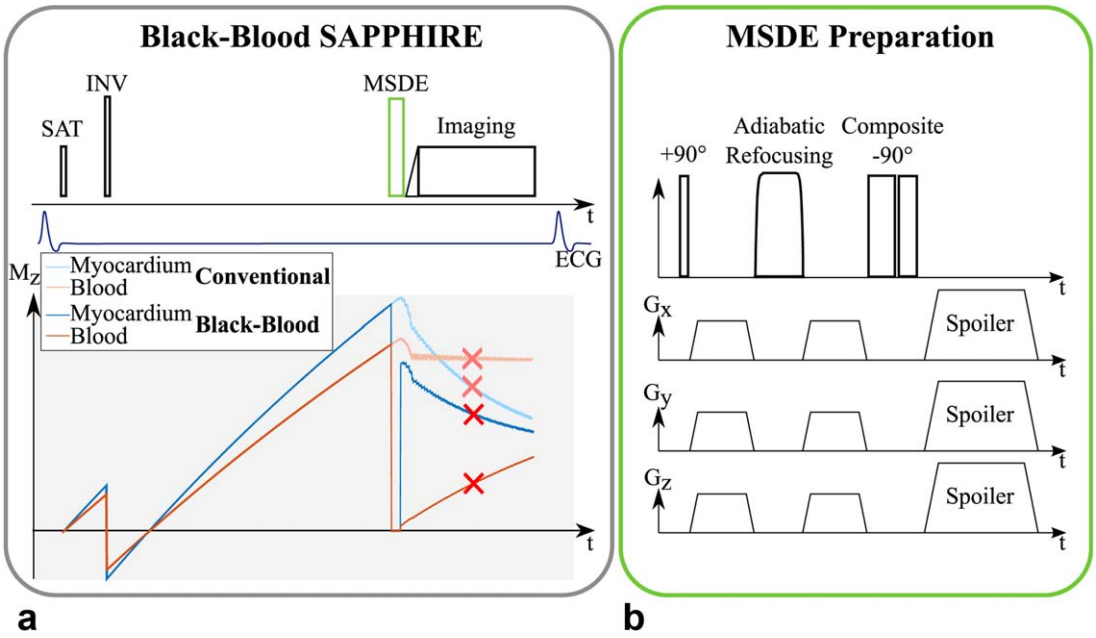

FIG. 1. (**a**) Sequence scheme of the proposed black-blood T_1 mapping method. As in conventional SAPPHIRE, a saturation pulse is played at the detection of the R wave, followed by an inversion pulse after a variable delay. For black-blood SAPPHIRE, an additional MSDE preparation is inserted right before the imaging pulses. (**b**) Sequence diagram of a MSDE preparation consisting of a tip-down, a refocusing, and a tip-up pulse. Strong motion-sensitizing gradients are inserted before and after the refocusing pulse.

METHODS

Sequence

Black-blood T_1 mapping was performed using a modified saturation pulse prepared heart-rate-independent inversion recovery (SAPPHIRE) (15) technique. A MSDE preparation was inserted directly before the balanced steady-state free-precession (bSSFP) imaging readout (Fig. 1a). In a MSDE preparation, a nonselective 90° tip-down pulse, a series of one or more 180° refocusing pulses, and a final 90° tip-up pulse are used to encode the spin dephasing in the longitudinal magnetization (Fig. 1b). Strong gradients with identical gradient moments are placed before and after the refocusing pulses to induce dephasing of differentially moving tissue.

Numerical Simulations

Numerical simulations of a bicompartment model have been performed to study the effect of partial voluming on the T_1 estimation in a SAPPHIRE sequence. A myocardial tissue compartment has been simulated with T_1/T_2 = 1580 ms/50 ms and a blood compartment with T_1/T_2 = 2300 ms/250 ms. In this noise-free simulation, the signal strength of the myocardial compartment, relative to the blood compartment, was chosen as the signal-to-noise ratios (SNR) for myocardium over the SNR of blood obtained from literature values (16): without MSDE: myocardium/blood = 117/119; with MSDE: myocardium/blood = 95/11. The relative compartmental share between blood and myocardium was varied between 0% and 100%. The overall signal of the SAPPHIRE sequence with and without MSDE preparation was simulated using the Bloch-equations. T_1 times were obtained by fitting a three-parameter model to the simulated signal intensities using a nonlinear Levenberg-Marquardt least-squares optimization (17).

To study the visual effects of partial voluming, a numerical representation of a cardiac short-axis slice was simulated with blood and myocardial compartments of the left and right ventricle. The numerical phantom was generated with a matrix size of 1024 × 1024 pixels and subsequently down-sampled using bilinear interpolation in order to induce partial voluming. Matrix sizes after down-sampling were chosen to correspond to approximate pixel resolutions of 1.5 × 1.5 to 3.0 × 3.0 mm^2. To facilitate comparability between different resolutions, all images were then up-sampled to a reconstruction resolution of 0.5 × 0.5 mm^2 prior to further processing. Bloch equations were used to simulate voxel-wise signals of the numerical phantom using the same myocardium and blood compartments as described above. Subsequent fitting with a three-parameter model was used to generate the T_1 maps.

Imaging

All imaging was performed on a 3T scanner (Magnetom Skyra; Siemens Healthcare, Erlangen, Germany) with a 30-channel receive array.

All T_1 mapping sequences have been performed with the following imaging parameters: repetition time/echo time (TR/TE) = 2.9/1.0 ms, flip angle = 45°, bandwidth = 1085 Hz/Px, field of view = 400 × 300 mm^2, in-plane resolution = 2.1 × 2.1 mm^2, partial Fourier = 6/8, GRAPPA 2, number of phase-encoding steps = 56. The flip angle was adjusted if specific absorption rate (SAR) limitations were reached.

In the present MSDE implementation the black-blood gradients were played out with all three gradient coils, maximum gradient amplitude of 20 mT/m per axis, and

a slew rate of 150 mT/m/ms leading to gradient ramp times of 0.14 ms. Motion-sensitizing gradient duration was maximized within the gaps between the respective tip-up/tip-down and the refocusing pulse. MSDE echo time was fixed to $TE_{MSDE} = 11$ ms, if not stated otherwise.

Phantom

Imaging has been performed in a static phantom to study B_1^+ uniformity of various MSDE preparation modules and to verify accuracy of the black-blood SAPPHIRE sequence.

The following three MSDE preparation modules with different combinations of radiofrequency (RF) pulses were tested for B_1^+ uniformity in a homogeneous phantom containing NaCl-doped water: 1) rectangular, 90° hard pulses for tip-down and tip-up and a single 180° MLEV refocusing pulse, as proposed in (16); 2) a rectangular 90° hard pulse for tip-down, an adiabatic 180° BIREF1 refocusing pulse, and a composite (270°–360°) tip-up pulse; and 3) a 0° three-compartment BIR4 pulse, with the MSDE gradients inserted symmetrically between the compartments (18,19). The timing of the RF pulses in the MSDE modules is detailed in Supporting Table S1. The echo time of the three MSDE modules was fixed to $TE_{MSDE} = 15$ ms. B_1^+ uniformity was assessed as the signal of a MSDE-prepared single-shot image, normalized by the signal of a single-shot image without MSDE preparation. The imaging parameters were as described above.

Furthermore, accuracy of the SAPPHIRE black-blood sequence was evaluated in phantom scans. The phantom was composed of seven vials containing agarose gel doped with various concentrations of gadoterate meglumine (Dotarem; Guerbet, Aulnay-sous-Bois, France) to achieve T_1 and T_2 times in the physiological range. The combination of composite pulses and the adiabatic refocusing was used for MSDE preparation in the remainder of the study. Conventional SAPPHIRE without MSDE preparation was performed as a reference. The T_1 times obtained with the SAPPHIRE black-blood sequence were compared to conventional SAPPHIRE using Bland-Altman analysis.

In Vivo

The study was approved by the local institutional review board, and written informed consent was obtained from all subjects prior to scanning.

The black-blood preparation was optimized in a cohort of five healthy subjects (3 male, 29 ± 4 years old). Baseline images without saturation/inversion preparation, as acquired in the SAPPHIRE black-blood sequence, were obtained with varying the echo time TE_{MSDE} from 10 ms to 14 ms. The effectiveness of blood suppression was quantitatively analyzed as the contrast-to-noise ratio (CNR) between the left ventricular myocardium and the left ventricular blood pool. To capture the effects of stagnant blood in the CNR, manually drawn endocardial contours covering the entire left ventricular blood pool were used for signal analysis of the blood. Signal heterogeneity in the myocardium, caused by the MSDE preparation, was quantitatively analyzed as the coefficient of variation (COV) of the signal over the entire myocardium between the epi- and the endocardial contours.

A separate cohort of eight healthy volunteers (4 male, 28 ± 4 years old) was recruited for T_1 time analysis. Imaging was performed using standard and black-blood SAPPHIRE in three short-axis slices and one four-chamber slice. T_1 times were evaluated using manually drawn regions of interest (ROIs). Average segmental T_1 times were assessed according to the American Heart Association (AHA) 6-segment model. Precision was obtained as the average intersegment variation. SNR of the baseline image without saturation/inversion preparation was analyzed for both sequences based on the signal of the two septal segments in the most basal slice over the standard deviation in a noise area corrected for the non-gaussian noise distribution. The average myocardial thickness was assessed between the manually drawn epi- and endocardial contours: 1000 spokes through the center of mass were uniformly spread around the myocardium. Thickness was then defined as the average distance of the crossing point of the spoke with the endo- and epicardial border, respectively. T_1 times, T_1 time precision, and average myocardial ROI thickness were compared between conventional and black-blood SAPPHIRE on a per subject basis using Student *t* test. *P* values < 0.05 were considered to be significant.

Partial voluming effects in the myocardium were visualized by analyzing the transmural T_1 times in five rings around the myocardium from the endo- to the epicardial border. The rings were divided in three segments around the myocardium (septal, antero-, and inferolateral). Average T_1 time per segment and per ring was then compared between conventional and black-blood SAPPHIRE.

Inter- and intraobserver variability was studied for black-blood and conventional T_1 mapping. Two readers drew a total of three ROI sets (reader 1: ROIs A, ROIs B, reader 2: ROIs C). Intraobserver variability was studied comparing the T_1 times obtained with ROIs A and ROIs B on a per subject basis. To obtain the interobserver variability, the per subject mean of the T_1 obtained with ROIs A and ROIs B (average of reader 1) were compared to ROIs C (reader 2). One subject, where segments had to be excluded due to bSSP imaging artifacts, was excluded from the consistency analysis to avoid reproducibility errors caused by differential artifact inclusion. Inter- and intraobserver consistency were analyzed using the interclass correlation coefficient (ICC) based on Winer's adjustment of anchor points (20,21). The ICCs between the two sequences were statistically compared for inter- and intraobserver analysis using F statistics. Absolute agreement in the inter- and intraobserver reproducibility was assessed according to Bland-Altman analysis (22). Paired *t* tests were used to assess differences in the bias between the two sequences, and F tests were used to analyze differences in the variance of the agreement. A significance level of $P < 0.05$ was used for all statistical tests, and consistency intervals are reported for a 95% level.

Furthermore, quantitative analysis of the in vivo partial voluming was performed by retrospective alteration of the manually drawn ROIs, as proposed in (10). The binary ROI masks were eroded or dilated by up to two and four pixels, respectively, in order to decrease/increase the myocardial ROI thickness. The average T_1 times in the five septal

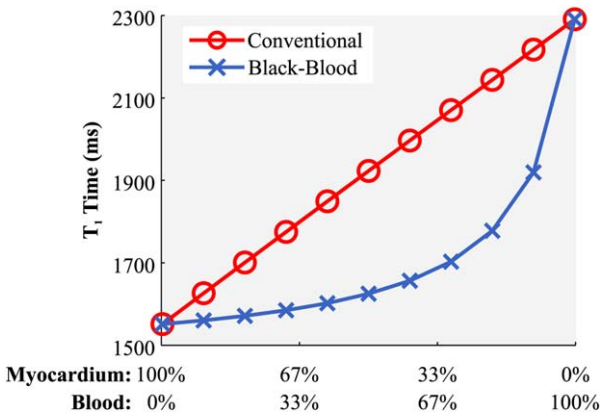

FIG. 2. Simulated T_1 time in a voxel, with partial voluming at varying signal contributions of blood and myocardium using conventional and black-blood SAPPHIRE. A linear increase of the T_1 time is observable with more blood contribution when using conventional SAPPHIRE. The blood–myocardial transition is substantially steepened using the proposed black-blood technique.

AHA segments, which are in the vicinity of both blood pools, were compared between conventional and black-blood SAPPHIRE at the various altered ROIs. Correlation between the septal T_1 time and the ROI thickness were identified using Pearson's correlation coefficient. Furthermore, one-way analysis of variance (ANOVA) was employed to test the T_1 times at various ROI thicknesses for differences in the mean to exclude nonlinear trends. P values < 0.05 were considered to be significant.

RESULTS

Numerical Simulations

Figure 2 shows the T_1 time in a simulated voxel with partial signal contribution of blood and myocardium. T_1 times assessed with conventional SAPPHIRE increases linearly with increased share of blood signal in the voxel. The black-blood approach successfully reduces the impact of blood signal in the voxel, leading to substantially steeper myocardial blood transitions.

The visual impact of this partial voluming reduction on the numerical phantom is depicted in Figure 3. Using conventional SAPPHIRE, apparent myocardial thickness reduces with coarser sampling resolution, creating smoothed edges at the blood–myocardial interface. This trend is also highlighted in the line plots: Coarse sampling leads to flat slopes toward the blood pool and a reduced width of the plateau with uncorrupted myocardial T_1 times. The black-blood preparation, on the other hand maintains steep slopes and a broad area with largely uncorrupted T_1 times, as apparent in the line plots (Fig. 3b). This leads to increased myocardial thickness in the numerical phantom.

Phantom

The results of the B_1^+ uniformity using three MSDE preparation modules are displayed in Figure 4. The BIR4 adiabatic module results in the least signal loss with the most homogeneous signal profile. The hybrid composite/BIREF1 module shows slightly increased signal loss with a signal drop toward the center of the phantom. This trend is strongly increased using the rectangular module. However, the relative SAR of the BIR4, composite/BIREF1, and the rectangular module were 9.6, 5.2, and 1.0, respectively. The composite/BIREF1 module was used for blood suppression as a tradeoff in the remainder of the study.

The Bland-Altman analysis of the phantom scans shows good agreement between the black-blood sequence and the conventional approach (see Supporting Figure S1): The average deviation was −3.9 ms (95% confidence interval [CI]: −15.4 ms to 7.6 ms) for phantom vials with T_1 times between 100 and 1800 ms.

In Vivo

Figure 5 shows the analysis of MSDE-prepared single-shot images acquired with various echo times (TE_{MSDE}). Residual blood signal is readily visible in the exemplary images if the echo time is chosen too short (10 ms), causing decreased CNR. However, progressively strong signal void in the lateral area of the myocardium can be observed with increasing echo times due to increased

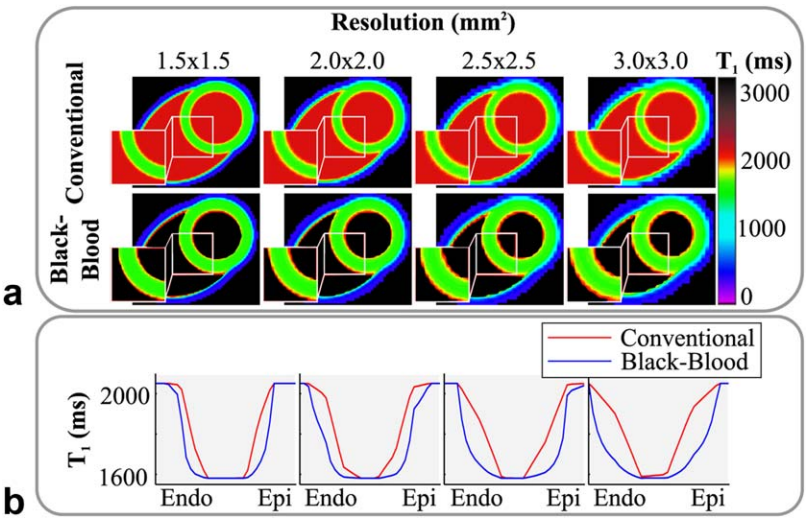

FIG. 3. (**a**) T_1 maps generated from numerical phantoms at various resolutions to obtain a varying degree of partial voluming. Decreased myocardial thickness can be observed with conventional T_1 mapping at coarser resolutions. Black-blood T_1 mapping mitigates this effect. (**b**) Line plots through the myocardium showing increasingly blurred blood–myocardium interfaces with conventional SAPPHIRE. Steep transitions are maintained using black-blood SAPPHIRE.

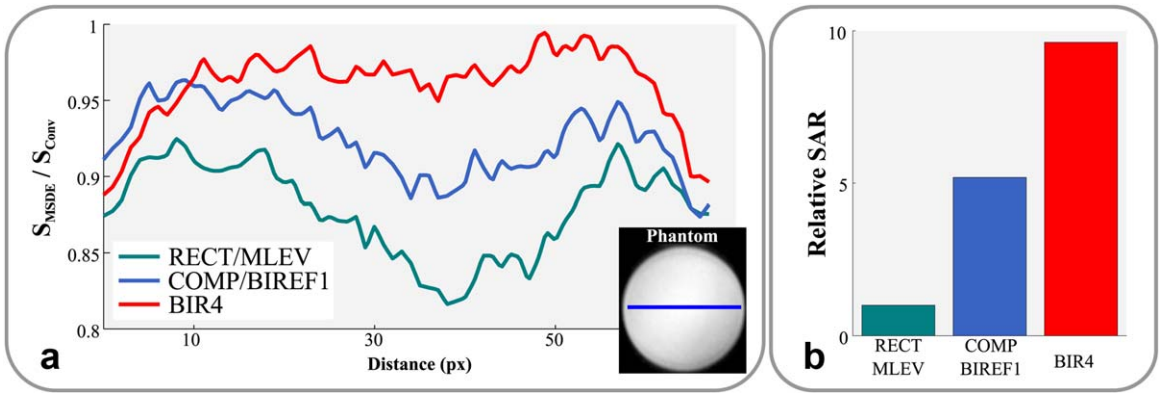

FIG. 4. (**a**) B_1^+ uniformity of three MSDE preparation modules shown as line plots in a homogeneous phantom. (**b**) Bar plots showing the relative SAR burden of the three modules. The BIR4 module shows the most uniform signal with the least signal loss for the cost of highest SAR values. The hybrid COMP/BIREF1 scheme shows a slight signal drop toward the center of the phantom. This trend is strongly increased using a fully rectangular preparation.

motion during the preparation. This reflects as increased signal heterogeneity in the myocardium (COV) and causes a CNR drop for long echo times. $TE_{MSDE} = 11$ ms shows substantially higher blood-myocardium contrast than shorter echo times, and reduced signal heterogeneity compared to long TE_{MSDE}. This echo-time value was fixed for the remainder of the study to offer a tradeoff between blood suppression and signal void.

T_1 mapping was successfully performed in all healthy subjects; two out of 136 (1.5%) segments of the black-blood T_1 maps were excluded from further analysis due to bSSFP artifacts. The imaging flip angle was reduced by 2° in one healthy subject due to SAR limitations. Representative T_1 maps acquired with conventional and black-blood SAPPHIRE are shown as myocardial overlays, together with the corresponding T_1-weighted baseline images in Figure 6. Good T_1 time homogeneity throughout the myocardium is observed with both techniques. Black-blood SAPPHIRE shows slightly increased variability by visual inspection. However, visually increased myocardial thickness is achieved with the black-blood sequence. The upper panel of Figure 6 shows the transmural analysis in a healthy subject and the corresponding T_1 map. Increased T_1 values are observed toward the blood pools with the conventional approach. No such elevation was seen using black-blood SAPPHIRE. Figure 7 depicts all baseline images used for the T_1 map generation, and the corresponding signal intensities in the myocardium and the blood pool, for the conventional and the black-blood sequence in one healthy subject. Black-blood SAPPHIRE shows comparable T_1 recovery curves to the conventional sequence in the myocardium, although at decreased intensity. Accordingly, the myocardial SNR in the baseline images of the conventional sequence was 76 ± 42% higher than with black-blood SAPPHIRE. The high-intensity blood signal in the conventional T_1 mapping sequence is successfully suppressed in the black-blood approach. However, the almost flat intensity curve in the blood pools of the black-blood sequence does not allow for extraction of the blood T_1 time.

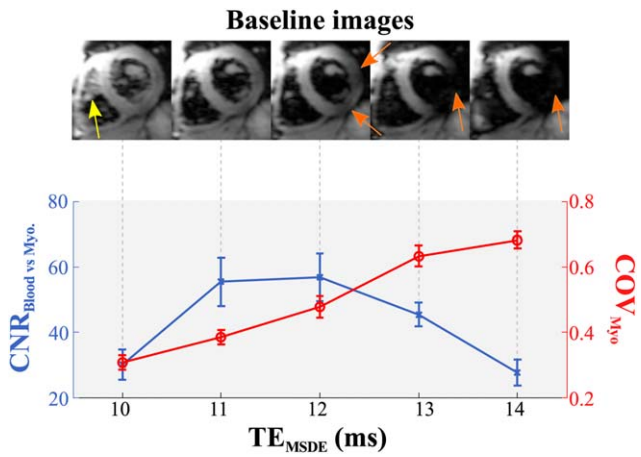

FIG. 5. Black-blood contrast as a function of the MSDE preparation echo time. Exemplary baseline images (upper panel) show residual blood signal for too short echo times (yellow arrow), whereas long echo times cause myocardial signal void (orange arrows). Accordingly, the contrast-to-noise ratio (CNR) between myocardium and blood pool is compromised for long and very short echo times. The coefficient of variation (COV) in the myocardium increases with longer echo times, caused by progressive signal void.

No significant difference was found between the average T_1 times of the conventional and the black-blood approach (1583 ± 58 ms vs. 1562 ± 56 ms, $P = 0.20$), with slightly lower T_1 time in the black-blood sequence, especially in the septal regions (Fig. 8). However, as assessed by intrasegmental T_1 variation, precision is significantly increased using the black-blood approach (63.1 ± 6.4 ms vs. 133.9 ± 24.6 ms; $P < 0.0001$). The myocardial thickness in SAPPHIRE black-blood T_1 maps was significantly increased by an average of 50% ± 22% compared to conventional SAPPHIRE, as detailed in Table 1.

Intraobserver consistency was characterized by an ICC of 0.939 (95% CI: [0.689, 0.989]) for the conventional sequence and an ICC of 0.979 (95% CI: [0.882, 0.996]) for the black-blood approach. This difference was not found to be significant ($P = 0.11$). Bland-Altman statistics showed slightly

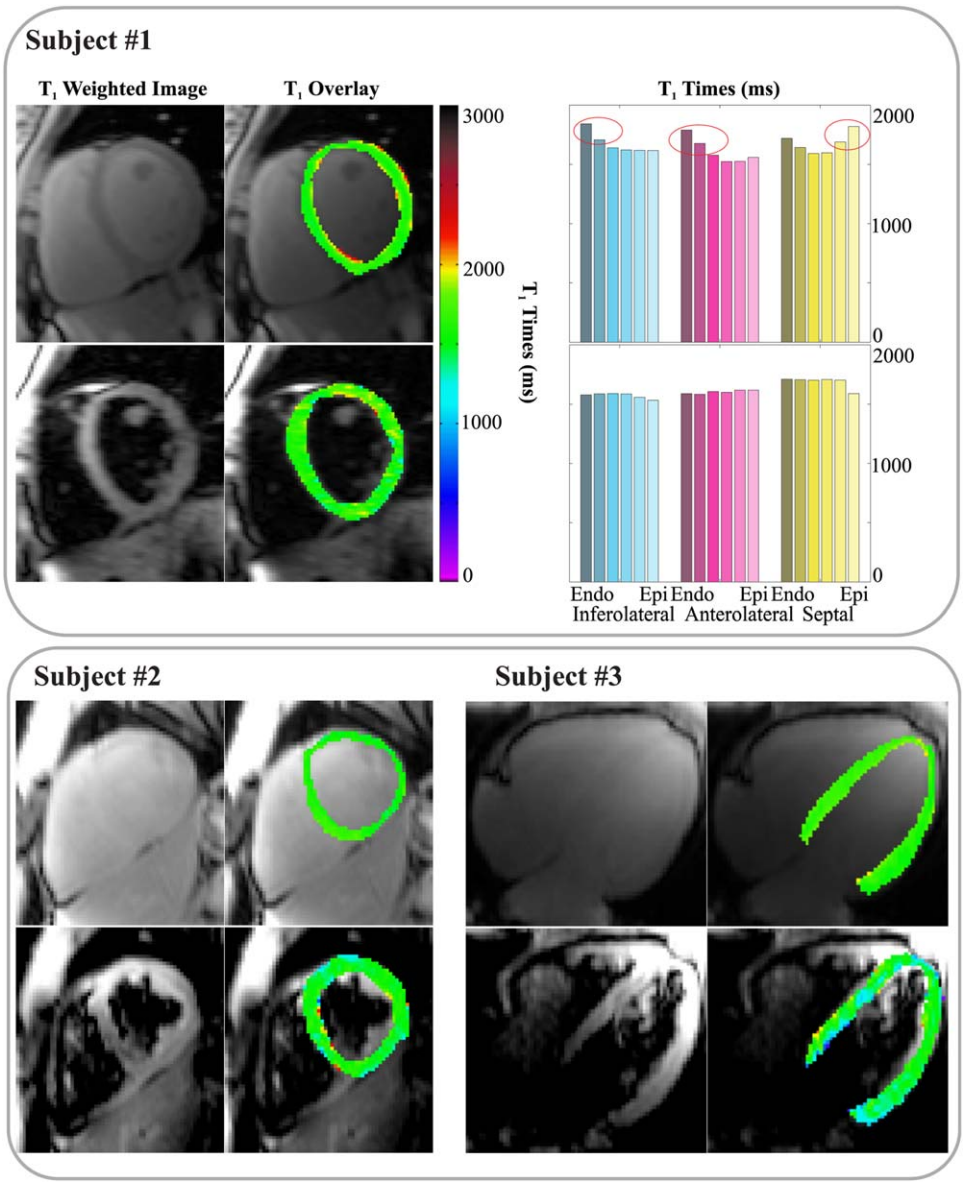

FIG. 6. T_1-weighted baseline images (left columns) and color-scaled myocardial T_1 map overlays (right columns) in three healthy subjects, acquired in short-axis or four-chamber orientation. Good homogeneity of the T_1 times is assessed with both techniques in all subjects. Slightly increased variability is visible in the black-blood approach. The analysis of the transmural T_1 times in subject 1 is shown in the upper right. Conventional T_1 mapping shows increased T_1 times at the blood–myocardial interface. No such elevation is observed with the black-blood technique.

lower intraobserver variability for the SAPPHIRE black-blood (bias: 1.3 ms, 95% CI: [−24.6, 27.3 ms]) compared with the conventional sequence (bias: −2.5 ms, 95% CI: [−37.7, 32.6 ms]). However, neither the difference in the bias ($P = 0.58$) nor in the variability of the differences ($P = 0.48$) was found to be significant. Interobserver consistency, on the other hand, was significantly lower using the conventional T_1 mapping sequence compared to black-blood SAPPHIRE (mean, [95% CI]): conventional 0.967, [0.822, 0.994] vs. black-blood: 0.996, [0.976, 0.999], $P = 0.011$. Also, significantly lower bias was shown for the proposed sequence in the Bland-Altman analysis (mean, [95% CI]): conventional −20.2 ms, [−46.5 ms, 6.0 ms] vs. black-blood: 1.3 ms, [−9.8 ms, 12.5 ms], difference in bias: $P = 0.003$, difference in variance: $P = 0.056$.

The quantitative analysis of the partial voluming, using erosion and dilation of the myocardial ROIs, is shown in Figure 9. Septal T_1 times assessed with conventional SAPPHIRE show a strongly increasing trend for dilated ROIs ($R^2 = 0.99$), with significantly different T_1 times at different ROI sizes ($P = 0.012$). SAPPHIRE black-blood shows good invariance to the ROI thickness over a wide range, with no increasing trend and no significant difference in the ANOVA ($R^2 = 0.29$, $P = 0.997$).

DISCUSSION

In this study, a MSDE-prepared SAPPHIRE sequence was proposed for blood signal-suppressed T_1 mapping. Numerical simulations showed that black-blood T_1 mapping benefits from decreased sensitivity to partial voluming effects and increased apparent myocardial wall thickness. Phantom T_1 times of black-blood SAPPHIRE were in good agreement with the conventional sequence. In vivo T_1 maps in healthy volunteers showed thorough blood suppression with the chosen MSDE module, and robust T_1 quantification in myocardial ROIs with increased thickness for the tradeoff against decreased

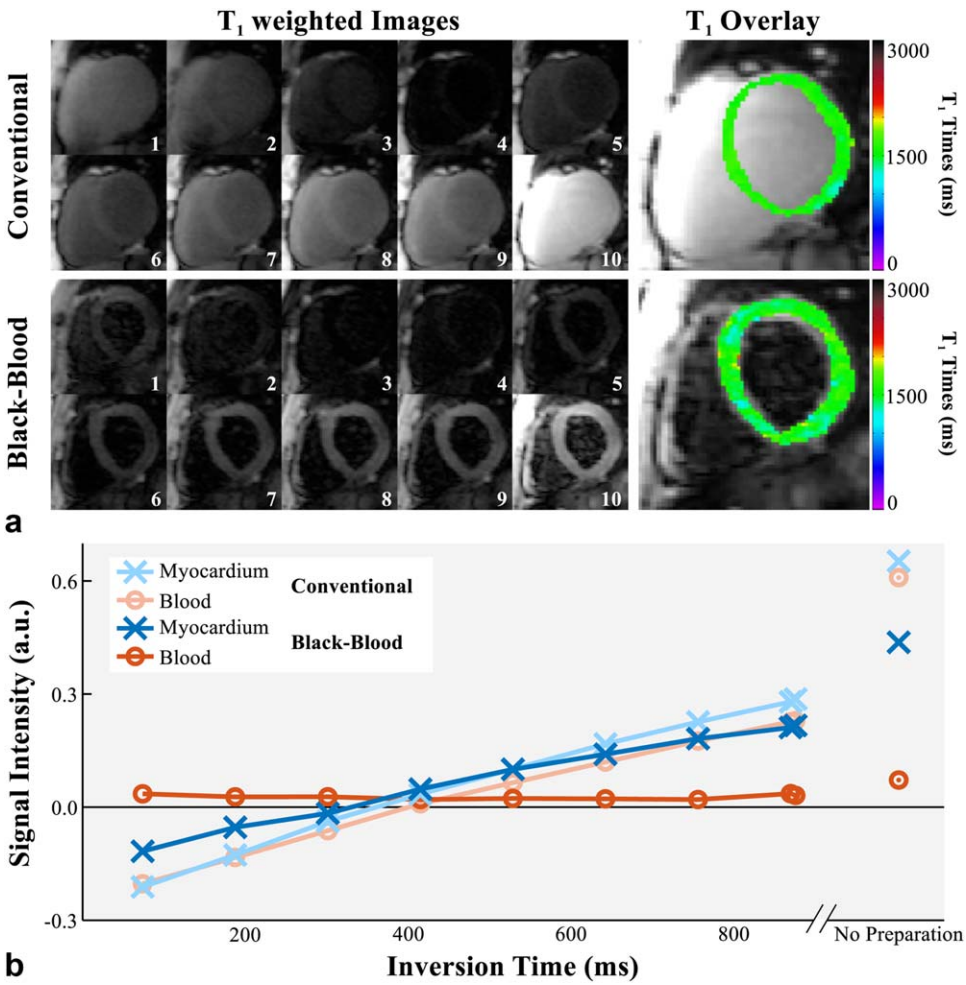

FIG. 7. (a) Series of T_1-weighted baseline images with different inversion times and the corresponding T_1 map overlay, as acquired in the conventional and black-blood SAPPHIRE T_1 mapping sequence in one healthy subject. (b) Signal intensities of the septal myocardium and the left-ventricular blood pool in the baseline images shown in (a). T_1 recovery curves are obtained in the myocardium with both sequences. The high blood signal in the conventional T_1 mapping sequence is successfully suppressed with the black-blood approach, leading to minor differences in the blood signal across the inversion times.

precision. Black-blood T_1 mapping successfully eliminated the T_1 time dependence on the ROI thickness and increased interobserver consistency, indicating the mitigation of partial voluming effects and high resilience to ROI alterations.

A MSDE preparation was employed for blood signal suppression in this study because it can be well integrated in a T_1 mapping sequence. Black-blood imaging using MSDE is clinically well established for plaque assessment in the coronary arteries (23). Active research efforts have focused on the optimization of MSDE preparations for plaque imaging (24–26). However, previous studies have shown substantial differences in the demands on the MSDE preparation for effective blood suppression in the left ventricle compared to the coronary arteries (16,27). Substantial differences in the flow patterns, with more shearing and less ordered motion in the left ventricle, require reduced motion-sensitizing gradient strength than for the coronary arteries: The optimal first-order gradient moment (m_1) was reported to be around ~160 mT · ms^2/m for ventricular applications (16,27) and 800 to 1,600 mT · ms^2/m for plaque imaging (25,28). Hence, to account for these differences and to ensure optimal blood suppression that meets the requirements of quantitative imaging, a separate optimization of the MSDE preparation and the motion-sensitizing gradient strength was performed. A hybrid adiabatic/composite preparation module was chosen as a tradeoff between B_1^+ uniformity and SAR that enables thorough blood suppression in the healthy volunteer cohort, suitable for quantitative imaging. The assessed optimal echo time (TE_{MSDE}) leads to a first-order gradient moment of $m_1 = 168$ mT · ms^2/m, which is in agreement with previous reports (27).

To enable optimal blood suppression with minimal signal void in the myocardium, careful positioning of the preparation at a time point with minimal contractile motion of the heart is necessary. Imaging was performed at late end-diastole in order to accommodate the MSDE preparation well within the end-diastolic quiescence. A fixed echo-time $TE_{MSDE} = 11$ ms showed consistent T_1 map quality in the healthy cohort. However, in patients with high heart rates or arrhythmias, cardiac motion during the MSDE preparation might be unavoidable and potentially detrimental to the image quality in the proposed black-blood approach. Patient-specific adaption of the MSDE preparation should be performed in these cases to achieve optimal image quality. TE_{MSDE} scouting has been previously proposed to enable efficient selection of the patient-specific optimal echo time (26). Also, alternative blood suppression schemes such as double-inversion recovery (29) or in-flow suppression (30)

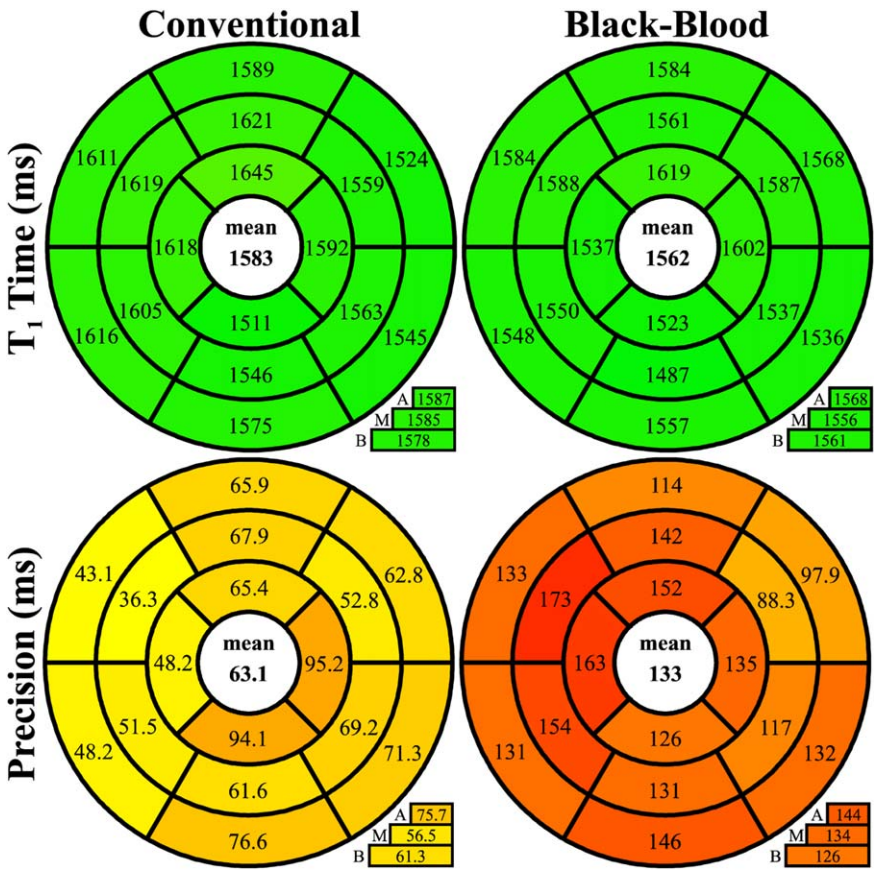

FIG. 8. Bulls-eye representation of T_1 times and precision in the 16 AHA segments across three slices (A = apical, M = midventricular, B = basal) acquired with conventional and black-blood SAPPHIRE. Similar T_1 times are assessed with both approaches, whereas significantly better precision is observed with conventional SAPPHIRE.

might be more suitable for patients with arrhythmia or tachycardia and warrant further inspection.

T_1 maps are commonly evaluated using manually drawn ROIs. However, especially in pathologies with reduced myocardial wall thickness, such as DCM or transmural scars, there are often only a few voxels left within the myocardium that are not affected by partial voluming (3). This bears the risk that elevated T_1 times in this cohort merely reflect a change in the extent of partial voluming. Black-blood T_1 mapping might be a valuable tool to confirm actual changes in the underlying myocardial T_1 in these pathologies, while eliminating the impairment by partial voluming effects.

Heng et al. recently presented initial data on the use of a MSDE-prepared fat-water separated T_1 mapping sequence (14). The sequence was based on a saturation recovery single-shot acquisition design (31) during free breathing. Although thorough blood suppression enabled good depiction of the right ventricle, the T_1 quantification with their pilot protocol was impaired by issues with robustness, reproducibility, and T_1 uniformity. The strong gradients in the MSDE preparation sensitize the magnetization even for small displacements. Hence, potential reasons for a lack of reproducibility in (14) include signal loss resulting from respiratory motion during free breathing, and suboptimal placement of the MSDE preparation due to the long multi-echo imaging readout. In the present study, rapid imaging during a breath hold mitigated these error sources and enabled reproducible T_1 mapping in the left ventricle. However, depiction of the right ventricle is hindered by the lack of fat-signal suppression. Initial results for fat-suppressed T_1 mapping has previously been proposed, showing high image quality using spectrally selective saturation of the fat before the imaging pulses (32). A combination of fat- and blood-suppressed T_1 mapping bears great promise for improved image quality and full elimination of partial voluming caused by epicardial fat, and it warrants further investigation.

Despite careful optimization of the MSDE module, a residual loss in precision was shown to be the major disadvantage of the proposed black-blood SAPPHIRE technique compared to the conventional T_1 mapping. The loss in T_1 mapping precision after the MSDE preparation can be attributed to multiple factors: 1) a consistent loss in SNR

Table 1
Average Myocardial ROI Thickness for Conventional and Black-Blood T_1 Mapping

Average Myocardial ROI Thickness (mm)			
SHAX Slice	Conventional	Black-Blood	Difference*
Apical	4.1 ± 0.7	6.2 ± 1.5	52% ± 24%
Mid	4.7 ± 1.1	7.3 ± 1.5	61% ± 33%
Basal	5.1 ± 0.8	6.8 ± 1.0	36% ± 22%
Average	4.6 ± 0.7	6.8 ± 0.8	50% ± 22%

*$P < 0.05$ for all differences.
ROI, region of interest.

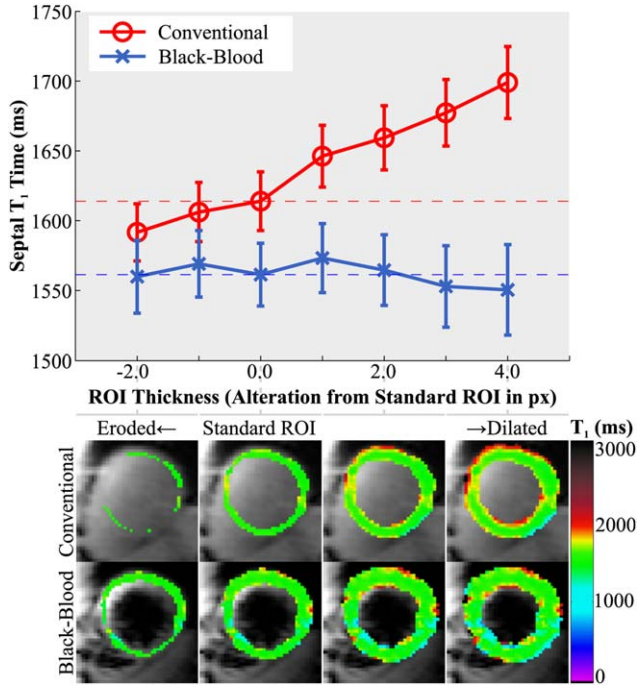

FIG. 9. Analysis of the in vivo partial voluming effect with conventional and black-blood SAPPHIRE. The upper panel shows the septal T_1 times at various alterations of the standard and manually drawn ROI obtained by progressive erosion/dilation. The lower panel shows the corresponding ROIs as color-scaled T_1 map overlays. Strongly increased T_1 times are observed at increased myocardial ROI thickness in the conventional technique due to the progressive inclusion of blood in the ROI. No such trend is observed using the SAPPHIRE black-blood sequence.

for all baseline images; 2) reduced resilience to imaging artifacts at lower SNR; and 3) increased variability among the baseline images. Our results indicate that the loss of the imaging SNR in the baseline images is the major source of increased variability. In addition to T_2 decay during the MSDE preparation, pulse imperfections and residual bulk motion of the myocardium reduce the signal after the preparation. Diffusion-related signal loss during the MSDE preparation can be assumed to be of minor importance due to very low b-values in the preparation (< 1 s/mm^2). Further loss in precision can be caused by increased susceptibility to imaging artifacts (e.g., fold-over) at lower SNR. Furthermore, additional variability among the baseline images can be induced in the proposed sequence due to differential patterns of residual motion in the myocardium.

The overall reproducibility in myocardial T_1 mapping is paramount and affected by a number of factors, including the T_1 mapping precision, the myocardial segment volume, and the inter- and intraobserver variability. On the one hand, reduced precision was shown for the proposed black-blood T_1 mapping technique compared with conventional SAPPHIRE. On the other hand, an increase in the readily evaluable myocardial area has been facilitated using blood suppression, allowing for increased segmental sizes and potentially reducing the variability of segmental T_1 times. Furthermore, the black-blood technique has shown high robustness toward variation of the ROI size. Correspondingly, our initial evaluation in a small cohort has indicated decreased interobserver variability with black-blood SAPPHIRE compared with the conventional sequence. Although these effects can be mitigated by observer training, this result is in line with a previous report on T_2^* mapping (33), showing that differential ROI delineation against the blood pool is a disruptive factor to the interobserver reproducibility. However, the differences in intraobserver variability were observed to be smaller, and no statistical significance was obtained given the small sample size. Hence, the assessment of the net overall effect on the reproducibility, inter- and intraobserver variability between black-blood, and conventional T_1 mapping requires a larger cohort to substantiate the claims and allow for statistical significant findings. This is to be evaluated in a future study.

Residual blood signal after the MSDE preparation was found to be insufficient for robust estimation of the blood T_1 time. This prevented the estimation of the extracellular volume (ECV) with the proposed technique. Because ECV estimation is the primary use of postcontrast T_1 times, the evaluation in the present work was restricted to the native myocardium, and no T_1 times after contrast injection were assessed. Separate assessment of a single, not spatially resolved blood T_1 time of the blood pool is potentially feasible with a rapid free-breathing technique (34). This will be evaluated as a supplement to the proposed technique in future studies in order to allow for black-blood ECV mapping.

This study and the proposed method have several limitations. Only a small number of healthy subjects were included in this proof of concept study, and no reproducibility or sensitivity toward pathological alternation in the T_1 time was assessed. Furthermore, the analysis of inter- and intraobserver variability was based on the assessments of two independent readers only. Increased consistency can be expected for larger cohorts due to learning effects on the readers or if common training is provided.

CONCLUSION

This study showed the feasibility of black-blood T_1 mapping at 3T. SAPPHIRE black-blood allows for accurate T_1 time quantification of the native myocardium that is robust to ROI alterations, and it eliminates partial voluming at the blood pools for the tradeoff against increased precision.

ACKNOWLEDGMENT

The authors would like to thank Dr. Peter Kellman for helpful discussions.

REFERENCES

1. Taylor AJ, Salerno M, Dharmakumar R, Jerosch-Herold M. T1 mapping: basic techniques and clinical applications. JACC Cardiovasc Imaging 2016;9:67–81.
2. Puntmann VO, Voigt T, Chen Z, Mayr M, Karim R, Rhode K, Pastor A, Carr-White G, Razavi R, Schaeffter T, Nagel E. Native T1 mapping in differentiation of normal myocardium from diffuse disease in hypertrophic and dilated cardiomyopathy. JACC Cardiovasc Imaging 2013;6:475–484.

3. Dass S, Suttie JJ, Piechnik SK, et al. Myocardial tissue characterization using magnetic resonance noncontrast t1 mapping in hypertrophic and dilated cardiomyopathy. Circ Cardiovasc Imaging 2012;5: 726–733.
4. Higgins DM, Ridgway JP, Radjenovic A, Sivananthan UM, Smith MA. T1 measurement using a short acquisition period for quantitative cardiac applications. Med Phys 2005;32:1738–1746.
5. Roujol S, Weingärtner S, Foppa M, Chow K, Kawaji K, Ngo LH, Kellman P, Manning WJ, Thompson RB, Nezafat R. Accuracy, precision, and reproducibility of four T1 mapping sequences: a head-to-head comparison of MOLLI, ShMOLLI, SASHA, and SAPPHIRE. Radiology 2014;272:683–689.
6. Kellman P, Hansen MS. T1-mapping in the heart: accuracy and precision. J Cardiovasc Magn Reson 2014;16:2.
7. Mehta BB, Chen X, Bilchick KC, Salerno M, Epstein FH. Accelerated and navigator-gated look-locker imaging for cardiac T1 estimation (ANGIE): Development and application to T1 mapping of the right ventricle. Magn Reson Med 2015;73:150–160.
8. Weingärtner S, Akcakaya M, Roujol S, Basha T, Stehning C, Kissinger KV, Goddu B, Berg S, Manning WJ, Nezafat R. Free-breathing post-contrast three-dimensional T1 mapping: volumetric assessment of myocardial T1 values. Magn Reson Med 2015;73:214–222.
9. Weingärtner S, Akcakaya M, Roujol S, Basha T, Tschabrunn C, Berg S, Anter E, Nezafat R. Free-breathing combined three-dimensional phase sensitive late gadolinium enhancement and T1 mapping for myocardial tissue characterization. Magn Reson Med 2015;74:1032–1041.
10. Ferreira VM, Wijesurendra RS, Liu A, Greiser A, Casadei B, Robson MD, Neubauer S, Piechnik SK. Systolic ShMOLLI myocardial T1-mapping for improved robustness to partial-volume effects and applications in tachyarrhythmias. J Cardiovasc Magn Reson 2015;17:77.
11. Coolen BF, Geelen T, Paulis LE, Nauerth A, Nicolay K, Strijkers GJ. Three-dimensional T1 mapping of the mouse heart using variable flip angle steady-state MR imaging. NMR Biomed 2011;24: 154–162.
12. Messner NM, Zöllner FG, Kalayciyan R, Schad LR. Pre-clinical functional magnetic resonance imaging part II: the heart. Z Med Phys 2014;24:307–322.
13. Koktzoglou I, Li D. Diffusion-prepared segmented steady-state free precession: application to 3D black-blood cardiovascular magnetic resonance of the thoracic aorta and carotid artery walls. J Cardiovasc Magn Reson 2007;9:33–42.
14. Heng EL, Kellman P, Gatzoulis MA, Moon J, Gatehouse P, Babu-Narayan SV. Pilot data of right ventricular myocardial T1 quantification by free-breathing fat-water separated dark blood saturation-recovery imaging. J Cardiovasc Magn Reson 2015:1–2.
15. Weingärtner S, Akcakaya M, Basha T, Kissinger KV, Goddu B, Berg S, Manning WJ, Nezafat R. Combined saturation/inversion recovery sequences for improved evaluation of scar and diffuse fibrosis in patients with arrhythmia or heart rate variability. Magn Reson Med 2014;71:1024–1034.
16. Srinivasan S, Hu P, Kissinger KV, Goddu B, Goepfert L, Schmidt EJ, Kozerke S, Nezafat R. Free-breathing 3D whole-heart black-blood imaging with motion sensitized driven equilibrium. J Magn Reson Imaging 2012;36:379–386.
17. Lourakis MIA. levmar: Levenberg-Marquardt nonlinear least squares algorithms in C/C++. Available at: http://users.ics.forth.gr/~lourakis/levmar/. Published 2004. Updated November 29, 2011. Accessed June 1, 2013.
18. Nezafat R, Ouwerkerk R, Derbyshire AJ, Stuber M, McVeigh ER. Spectrally selective B1-insensitive T2 magnetization preparation sequence. Magn Reson Med 2009;61:1326–1335.
19. Salerno M, Epstein FH, Kramer CM, inventors; Motion-attenuated contrast-enhanced cardiac magnetic resonance imaging and related method thereof. US Patent 12,696,433. January 29, 2009.
20. Winer BJ. Statistical principles in experimental design. New York, NY: McGraw-Hill; 1971.
21. Shrout PE, Fleiss JL. Intraclass correlations: uses in assessing rater reliability. Psychol Bull 1979;86:420–428.
22. Bland JM, Altman DG. Statistical methods for assessing agreement between two methods of clinical measurement. Lancet 1986;1:307–310.
23. Kerwin WS, Canton G. Advanced techniques for MRI of atherosclerotic plaque. Top Magn Reson Imaging 2009;20:217–225.
24. Wang J, Yarnykh VL, Hatsukami T, Chu B, Balu N, Yuan C. Improved suppression of plaque-mimicking artifacts in black-blood carotid atherosclerosis imaging using a multislice motion-sensitized driven-equilibrium (MSDE) turbo spin-echo (TSE) sequence. Magn Reson Med 2007;58:973–981.
25. Wang J, Yarnykh VL, Yuan C. Enhanced image quality in black-blood MRI using the improved motion-sensitized driven-equilibrium (iMSDE) sequence. J Magn Reson Imaging 2010;31: 1256–1263.
26. Fan Z, Zhou X, Bi X, Dharmakumar R, Carr JC, Li D. Determination of the optimal first-order gradient moment for flow-sensitive dephasing magnetization-prepared 3D noncontrast MR angiography. Magn Reson Med 2011;65:964–972.
27. Nguyen TD, de Rochefort L, Spincemaille P, Cham MD, Weinsaft JW, Prince MR, Wang Y. Effective motion-sensitizing magnetization preparation for black-blood magnetic resonance imaging of the heart. J Magn Reson Imaging 2008;28:1092–1100.
28. Balu N, Yarnykh VL, Chu B, Wang J, Hatsukami T, Yuan C. Carotid plaque assessment using fast 3D isotropic resolution black-blood MRI. Magn Reson Med 2011;65:627–637.
29. Edelman RR, Chien D, Kim D. Fast selective black-blood MR imaging. Radiology 1991;181:655–660.
30. Felmlee JP, Ehman RL. Spatial presaturation: a method for suppressing flow artifacts and improving depiction of vascular anatomy in MR imaging. Radiology 1987;164:559–564.
31. Chow K, Flewitt JA, Green JD, Pagano JJ, Friedrich MG, Thompson RB. Saturation recovery single-shot acquisition (SASHA) for myocardial T(1) mapping. Magn Reson Med 2014;71:2082–2095.
32. Peters DC, Thorn SL, Bregazi A, Hawley C, Stacy MR, Sinusas AJ. Towards high-resolution fat-suppressed T1-mapping of atrial fibrosis in the left atrium: a fit-free three-point method. J Cardiovasc Magn Reson 2015;17:1–2.
33. He T, Gatehouse PD, Kirk P, Tanner MA, Smith GC, Keegan J, Mohiaddin RH, Pennell DJ, Firmin DN. Black-blood T2* technique for myocardial iron measurement in thalassemia. J Magn Reson Imaging 2007;25:1205–1209.
34. Fitts M, Breton E, Kholmovski EG, Dosdall DJ, Vijayakumar S, Hong KP, Ranjan R, Marrouche NF, Axel L, Kim D. Arrhythmia insensitive rapid cardiac T1 mapping pulse sequence. Magn Reson Med 2013;70:1274–1282.

SUPPORTING INFORMATION

Additional supporting information may be found in the online version of this article.

Sup. Table S1. Summary of the three MSDE modules, with the employed RF pulses and corresponding timing.

Sup. FIG. S1. Bland-Altman analysis of phantom T_1 times assessed with conventional and black-blood SAPPHIRE. TE_{MSDE}=11ms was used in the black-blood sequence. Good agreement with minimal average deviation is shown between the two sequences.